

## Localization and quantization in covalently bonded carbon nanotube junctions

Fabrizio Cleri\*

*Ente Nuove Tecnologie, Energia e Ambiente (ENEA), Unità Materiali e Nuove Tecnologie,  
Centro Ricerche Casaccia, 00100 Roma A. D., Italy*

Pawel Keblinski

*Department of Materials Science and Engineering, Rensselaer Polytechnic Institute, Troy, New York 12180-3590, USA*

Inkook Jang and Susan B. Sinnott

*Department of Materials Science and Engineering, University of Florida, Gainesville, Florida 32611-6400, USA*

(Received 30 January 2004; published 25 March 2004)

A tight-binding Hamiltonian is used to study the electronic properties of covalently bonded, crossed (5,5) metallic nanotubes with an increasing degree of disorder in the junction region. Ideal junctions with a few topological defects show Ohmic behavior. Upon increasing disorder, Ohmic conduction is suppressed in favor of hopping conductivity. Strongly disordered junctions as could be obtained after electron-beam irradiation of overlaid nanotubes, display weak localization and energy quantization, indicating the formation of a quantum dot contacted to metallic nanowires by tunnel barriers.

DOI: 10.1103/PhysRevB.69.121412

PACS number(s): 61.46.+w, 71.23.An, 73.21.La

Carbon nanotubes (CNTs) have been proposed as a main component of future nanoscale electronics, either as fully active circuit elements in the form of linear, Y-shaped, or T-shaped heterojunctions,<sup>1-3</sup> or as interconnects in molecular-level devices.<sup>4</sup> Such extended capabilities are made possible by the fascinating electronic properties of CNTs, which can behave either as metals or semiconductors as a function of their molecular symmetry.

Junctions between CNTs are a key factor in the design of such nanoscale integrated devices. In particular, the properties of crossed nanotube junctions bonded by van der Waals interactions have been already investigated in some detail by both experimental and theoretical methods.<sup>5-7</sup> Conduction in such weakly coupled junctions occurs purely by tunneling, as determined by two- and four-terminal measurements aimed at factoring out the effect of the large contact resistance between the CNT and the metallic electrodes.<sup>8,9</sup> A different, and much less understood, situation is encountered in the strongly coupled, covalently-bonded junctions obtained by, e.g., electron-beam irradiation of crossed CNTs.<sup>10,11</sup> In this case, a whole range of electrical conduction mechanisms—from purely Ohmic to phonon-assisted hopping to quantum tunneling—is expected depending on both the electrical properties of pristine nanotubes and the nature of the covalent bonds formed upon irradiation.

In the present work, we investigate the electronic properties of covalently bonded (“e-beam welded”) crossed-CNT junctions by means of tight-binding molecular dynamics (TBMD) simulations, based on a well-established orthogonal TB model for carbon.<sup>12</sup> We calculate and analyze the local density of states (LDOS) and localization coefficient (“participation ratio”) for a number of different atomic structures. We find that an “ideal” junction between two coplanar (5,5) CNTs with a small concentration of defects should display a substantially Ohmic behavior. On the other hand, covalently bonded junctions between overlaid (5,5) CNTs at about 1.5–0.5 Å intertube distance, connected by an increasing

number of covalent bonds, display an increasing number of defect-induced electronic states around the Fermi energy  $E_F$ ; such states perturb and eventually suppress the Ohmic conduction, allowing for an increasing role of hopping conduction between localized states.

The most interesting behavior, however, is represented by the strongly disordered junctions obtained by a simulated electron-beam irradiation welding. In this case the spectrum around  $E_F \pm 0.5$  eV is composed of quantized levels weakly localized over the whole junction region, thus giving rise to a quantum dot (QD). Such an all-carbon QD structure appears very promising for several applications. It should be experimentally realizable by manipulating CNTs with the tip of an atomic-force microscope over properly arranged metallic contacts, and by subsequently irradiating the junction region as demonstrated in Refs. 10 and 11 to create a single QD, pairs of coupled QDs, and, eventually, arrays of regularly spaced QDs by means of tailored CNT-growth techniques.<sup>13</sup>

In all our studies we used an orthogonal TB model<sup>12</sup> including four valence orbitals  $\{s, p_x, p_y, p_z\}$  for each C atom. The electronic structure is obtained by analyzing the eigenvector spectrum  $c^{(n)}$  for the eigenvalues  $\epsilon^{(n)}$ ,  $n \in 4N$ , with  $N$  the number of C atoms and  $4N$  the number of electrons in the supercell. The partial sum  $\sum_n |c_\alpha^{(n)}(r_i)|^2$  is proportional to the probability density (“amplitude of the wave function”) of the orbital  $\alpha$  at the atomic site  $r_i$ , subject to the closure rule  $\sum_n \sum_{i,\alpha} |c_\alpha^{(n)}(r_i)|^2 = 4N$ . The participation ratio, proportional to the second moment (mean) of the probability density, is defined as

$$P^{(n)} = 4N \sum_{i,\alpha} |c_\alpha^{(n)}(r_i)|^4, \quad (1)$$

the sum running over all sites  $r_i$  and orbitals  $\alpha$ . Its deviation from the ideal value  $(4N)^{-1}$  gives an overall measure of the localization of the  $n$ th eigenvalue.

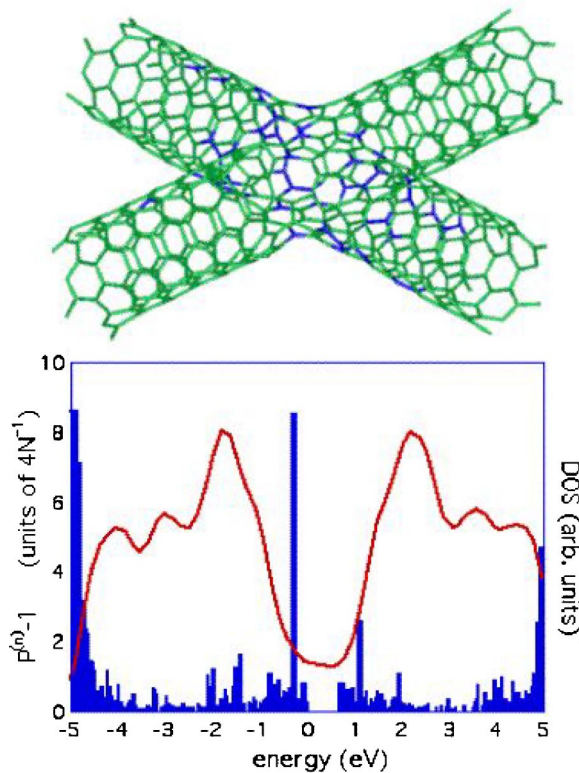


FIG. 1. (Color online) Top panel: Relaxed atomic structure of the junction obtained by crossing two coplanar (5,5) carbon nanotubes. Bottom: DOS (full curve) and eigenvalue participation ratio (histogram) around the Fermi level (shifted at  $E=0$ ).

In the following, we will discuss the simulation results for three representative covalent junction configurations, displaying purely Ohmic conduction, hopping-dominated charge transport, and QD behavior with tunnel barriers, respectively. We start by describing the relaxed atomic and electronic structure of an ideal junction between two coplanar (5,5) CNTs, with a diameter of 0.67 nm each. The system is periodic in the  $x$  and  $y$  directions and practically infinite along  $z$ . Two interpenetrating (5,5) CNT segments of 32 units each (corresponding to a length of about 3.9 nm between two periodic images of the junction along both  $x$  and  $y$ ) are placed in the  $z=0$  plane, with the cylinder axis parallel to the  $x$  and  $y$  directions, respectively. When two atoms are closer than 1.2 Å, one is removed by construction. The final atomic configuration, containing 568 C atoms, was relaxed by TBMD at  $T=0$  K, the resulting structure being shown in Fig. 1(a). The junction is asymmetric, i.e., all the connections between the four branches of the (5,5) CNTs are different from each other. Overall, the junction region contains two twofold-coordinated C atoms, six octagonal rings, four heptagonal rings, and two pentagonal rings.

In Fig. 1(b), we show the total DOS of the coplanar junction (full curve) and the participation ratio  $P^{(n)}$  (histogram) around the Fermi level  $E_F=0$  eV. The DOS remains quite flat around the Fermi level. No sign of localization is apparent for an extent of about 0.5 eV above  $E_F$ , while a moderate localization is seen for a few “shallow” states lying immediately below  $E_F$ . This implies that the structural defects

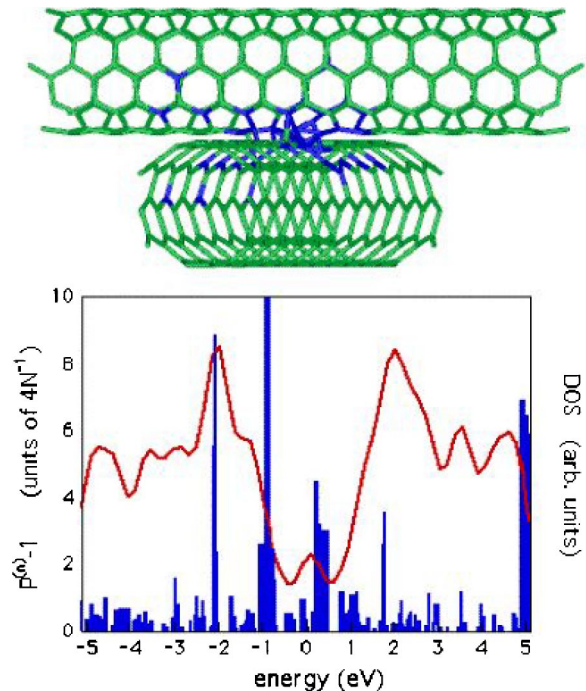


FIG. 2. (Color online) Top panel: Relaxed atomic structure of the junction obtained by crossing two overlaid (5,5) carbon nanotubes at a vertical distance of 0.5 Å. Bottom: DOS (full curve) and eigenvalue participation ratio (histogram) around the Fermi level (shifted at  $E=0$ ).

induce only a moderate perturbation on the conduction-electron wave functions. Moreover, if we cut away from the junction those sites at which the shallow states are mostly localized, the atomic structure still preserves several connecting paths across all four branches of the cross. These paths, by contrast, support fully extended electronic states, meaning that a good Ohmic conduction is preserved in the coplanar CNT junction even in the presence of a moderate concentration of topological and coordination defects.

We now describe a covalent junction obtained by crossing two overlaid (5,5) CNTs of length 2.95 nm each (24 units), placed at  $z=0$  and parallel to the  $x$  axis, and at  $z=+7.2$  Å and parallel to the  $y$  axis, respectively. The initial intertube distance is, therefore, about 0.5 Å. Three atoms were removed from the junction since they were too close to each other. After the structural relaxation of both the atomic positions and the supercell shape, the junction [Fig. 2(a)] contains three heptagonal rings and 14 fourfold-coordinated C atoms, all with bond angles largely distorted with respect to an ideally tetrahedral  $sp^3$  bonding.

In Fig. 2(b), we show the DOS of the overlaid junction (full curve) and the participation ratio  $P^{(n)}$  (histogram) in the interval  $E_F \pm 5$  eV. In this case, the DOS shows a distinct peak around the Fermi energy, corresponding to a whole set of strongly localized states including the eigenvalue at  $E=0$ . Practically all such localized states originate from the fourfold-coordinated sites connecting the two CNTs. In this kind of junction, therefore, Ohmic conduction is suppressed and the only viable transport mechanism should be phonon-assisted hopping across localized states.

In our previous work on diamond grain boundaries,<sup>14</sup> we formulated a multiphonon hopping model for charge transport in a mixed  $sp^2$ - $sp^3$  carbon network. By applying that same model to the present case, we can estimate the conductivity of the junction compared to that of the perfect (5,5) CNT. We recall that in a weak-coupling multiphonon model, the diffusion coefficient is given by<sup>15</sup>

$$D = \frac{1}{6} R^2 \nu_0 e^{-\gamma p} e^{-2R/\alpha} \left( \frac{k_B T}{h \nu_0} \right)^p, \quad (2)$$

where  $\nu_0 \cong 1.5$  THz is the average frequency of the phonon band most effectively coupled to localized electrons,  $R = 0.5$  Å is the average hopping distance, and  $\alpha = 6.5$  Å is the exponential decay length of the localized orbitals in carbon. The quantity  $p = \Delta/h\nu_0$ , with  $\Delta \cong 0.25$  eV the main energy shift, represents the average number of phonons involved in a hop from  $E_F$  to the first localized state. The quantity  $\gamma = \ln(\Delta/E_M) - 1$  describes electron-phonon coupling with  $E_M \cong 0.2h\nu_0$  (Ref. 14) the coupling constant. By inserting into Eq. (2) the numerical values obtained from our TB model, we get a negligible carrier diffusivity at any temperature, mostly because of the quite large first-level spacing  $\Delta$ . It is possible that hopping conductivity could increase to appreciable values in a junction with a higher density of defects.

Finally, we describe the atomic and electronic structure of a more “realistic” junction, as could be obtained after electron-beam irradiation of two crossed CNTs. As in the previous junction configuration, two segments of (5,5) CNTs containing 340 atoms each were overlaid at a wall-to-wall distance of about 3 Å along the  $z$  axis. In this case, however, a simulated electron-beam irradiation procedure was first carried out by combined microcanonical and Langevin molecular dynamics with a Tersoff-Brenner empirical potential.<sup>16</sup> The resulting atomic configuration was subsequently relaxed by TBMD. The final junction appears highly disordered [see Fig. 3(a)], with a sort of amorphouslike particle embedded within four CNT arms. Such a junction includes a large number of miscoordinated atoms, and several fourfold, fivefold, sevenfold, and eightfold rings.

The electronic structure of this kind of junction, shown in Fig. 3(b) (full curve) together with the participation ratio  $P^{(n)}$  (histogram), is quite surprising. A whole band around the Fermi level is localized at the junction region. All the energy levels are quantized within the junction, although being finely spaced by  $\Delta E \approx 10$ –50 meV. Such levels are defect states, but are weakly localized (i.e., spread) over the whole of the junction sites, while not belonging to the rest of the system. This can be clearly seen by plotting the quantity  $\sum_\alpha |c_\alpha^{(n)}(x_i)|^2$  as a function of the distance  $x_i$ , spanning either major axis of the cross. Figure 4 reports such plots for the first few eigenvalues of the discrete spectrum ( $n = 1, \dots, 8$ ) above the Fermi level ( $n = 0$ ). For  $n = 0, 1$ , the wave function is moderately localized, and spreads over a large part of the CNT arms. On the other hand, for  $n \geq 2$  the wave functions are substantially different from zero only in the junction region, in some cases being more strongly localized just at a few atomic sites. Such a combination of energy

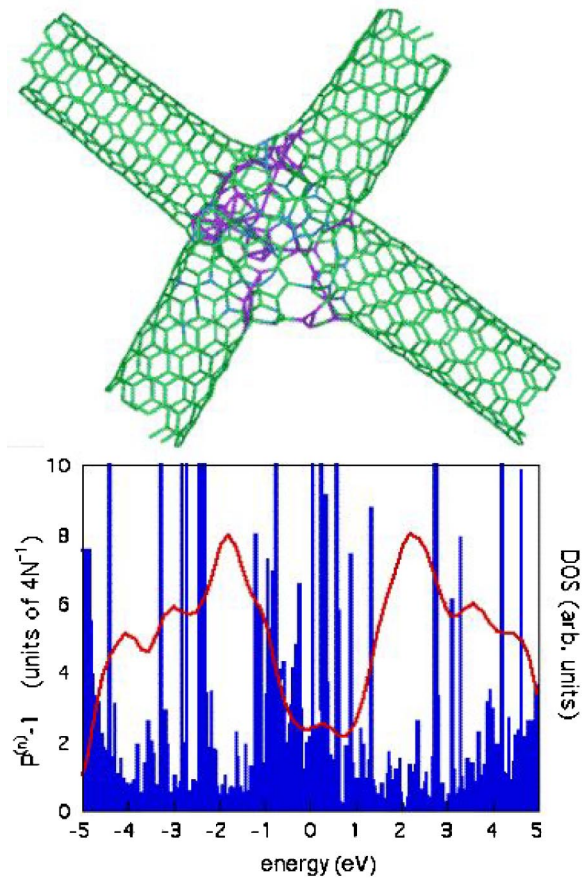


FIG. 3. (Color online) Top panel: Relaxed atomic structure of the junction obtained by simulating the electron-beam irradiation of two overlaid (5,5) carbon nanotubes. Bottom: DOS (full curve) and eigenvalue participation ratio (histogram) around the Fermi level (shifted at  $E = 0$ ).

quantization and weak spatial localization is the typical signature of a QD. Moreover, by looking at the LDOS (obtained by projecting the total DOS on selected subsets of atomic sites) it can be seen that the first few carbon rings immediately adjacent to the QD show a forbidden band of states immediately above  $E_F$ , i.e., these rings behave as tunnel barriers between the junction and the adjoining perfect-CNT branches.

The above results suggest that by combining nanomanipulation techniques and electron irradiation of CNTs, arrays of all-carbon-based QDs as small as 1 nm, spaced by 5–10 nm, could be obtained. Such QDs would be connected to ballistic conductors (the CNT arms) by construction, separated by a tunnel-barrier gate possibly allowing quantized charge injection into the QD. The junction region would be made chemically inert by saturation with hydrogen, which should not, however, alter its basic QD behavior. The application capabilities of such all-carbon nanoelectronic devices as building blocks of more complex molecular-scale electronic circuits should be immediately evident. For example, reactive substitution of hydrogen with organic radicals should be feasible to explore possible connections with the domain of electronically active molecules contacted to QD arrays.

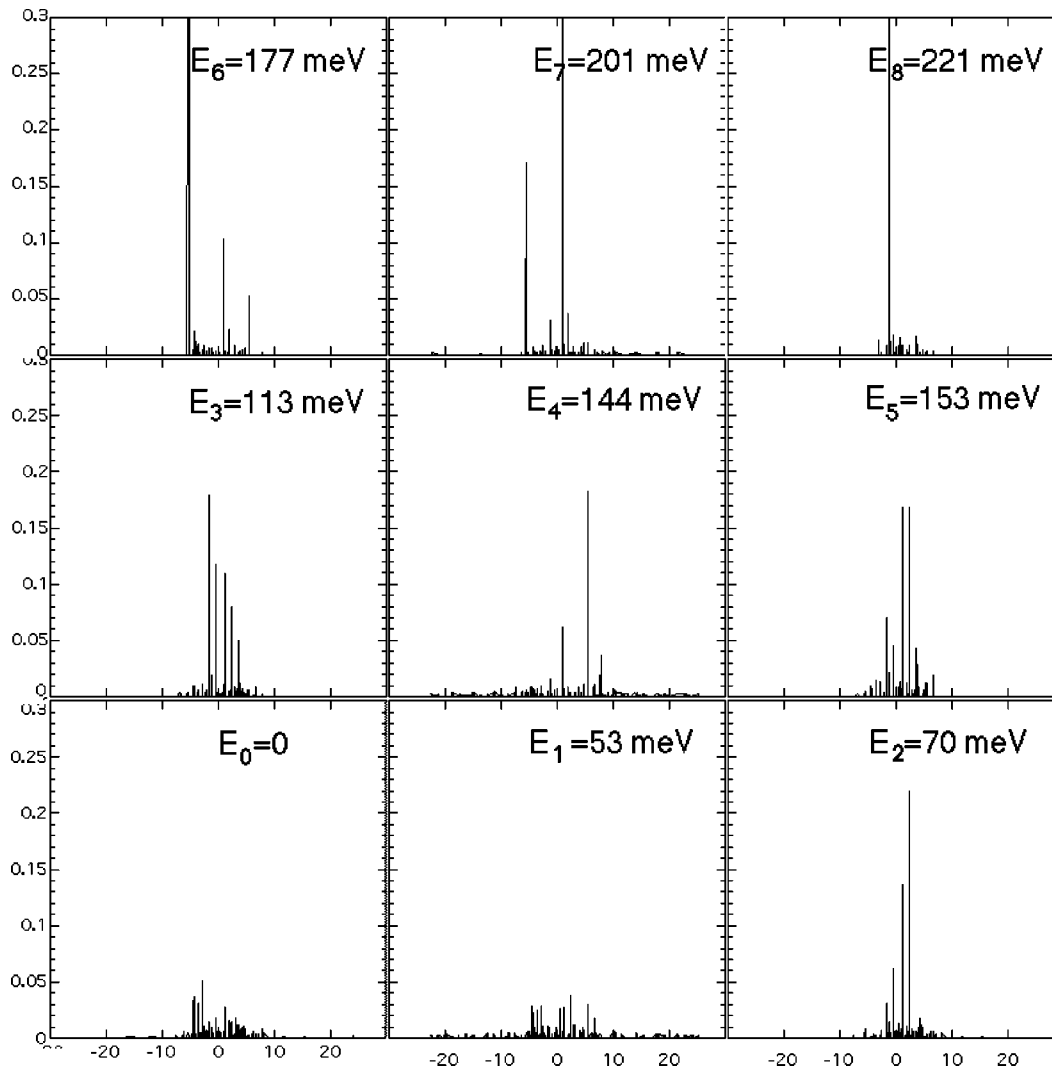


FIG. 4. Plot of the longitudinal distribution of the electron probability density,  $\sum_{\alpha} |c_{\alpha}^{(n)}(x)|^2$ , for the first few eigenvalues ( $n=0, \dots, 8$ ) above the Fermi level ( $n=0$ ) of the same nanotube junction of Fig. 3. The abscissa  $x$  spans either of the major tube axes. The junction region lies approximately between  $x = -5 \text{ \AA}$  and  $x = +5 \text{ \AA}$ .

F.C. thanks RPI for hospitality and generous support during a short-term visit. Discussions with Professor R. Raimondi (University RomaTre) are much appreciated. S.B.S.

acknowledges the support of the NSF Grant No. CHE-0200838. The work of P.K. was supported by the NSF Grant No. DMR134725.

\*Email address: cleri@casaccia.enea.it

<sup>1</sup>S. J. Tans, A. R. M. Verschueren, and C. Dekker, *Nature (London)* **393**, 49 (1998).

<sup>2</sup>Z. Yao, H. W. C. Postma, L. Balents, and C. Dekker, *Nature (London)* **402**, 273 (1999).

<sup>3</sup>Y.-G. Yoon, M. S. C. Mazzoni, H. J. Choi, J. Ihm, and S. G. Louie, *Phys. Rev. Lett.* **86**, 688 (2001).

<sup>4</sup>P. W. Chiu, G. S. Duesberg, U. Dettlaff-Weglikowska, and S. Roth, *Appl. Phys. Lett.* **80**, 3811 (2002).

<sup>5</sup>M. S. Fuhrer, J. Nygard, L. Shih, M. Forero, Y.-G. Yoon, M. S. C. Mazzoni, H. Joon Choi, J. Ihm, S. G. Louie, A. Zettl, and P. L. McEuen, *Science* **288**, 494 (2000).

<sup>6</sup>T. Rueckes, K. Kim, E. Joselevich, G. Y. Tseng, C.-L. Cheung, and C. M. Lieber, *Science* **289**, 94 (2000).

<sup>7</sup>H. W. Ch. Postma, M. de Jonge, Z. Yao, and C. Dekker, *Phys. Rev. B* **62**, 10 653 (2000).

<sup>8</sup>A. Buldum and J. P. Lu, *Phys. Rev. B* **63**, 161403 (2001).

<sup>9</sup>P. J. de Pablo, C. Gómez-Navarro, J. Colchero, P. A. Serena, J. Gómez-Herrero, and A. M. Barò, *Phys. Rev. Lett.* **88**, 036804 (2002).

<sup>10</sup>F. Banhart, *Nano Lett.* **1**, 329 (2001).

<sup>11</sup>M. Terrones, F. Banhart, N. Grobert, J.-C. Charlier, H. Terrones, and P. M. Ajayan, *Phys. Rev. Lett.* **89**, 075505 (2002).

<sup>12</sup>C. H. Xu, C. Z. Wang, C. T. Chan, and K. M. Ho, *J. Phys.: Condens. Matter* **4**, 6047 (1992).

<sup>13</sup>B. Q. Wei, R. Vajtai, Y. Jung, J. Ward, R. Zhang, G. Ramanath, and P. M. Ajayan, *Nature (London)* **416**, 495 (2002).

<sup>14</sup>F. Cleri, P. Keblinski, L. Colombo, D. Wolf, and S. R. Phillpot, *Europhys. Lett.* **46**, 671 (1999).

<sup>15</sup>D. Emin, *Adv. Phys.* **24**, 305 (1975).

<sup>16</sup>I. Jang, S. B. Sinnott, D. Danailov, and P. Keblinski, *Nano Lett.* **4**, 109 (2004).